



1 **Carbon-climate feedback higher when assuming Michaelis-** 2 **Menten kinetics of respiration**

3 Christian Beer^{1, 2}

4 ¹Department of Earth System Sciences, Universität Hamburg, Hamburg, 20134, Germany

5 ²Center for Earth System Research and Sustainability, Universität Hamburg, Hamburg, 20134, Germany

6 *Correspondence to:* Christian Beer (christian.beer@uni-hamburg.de)

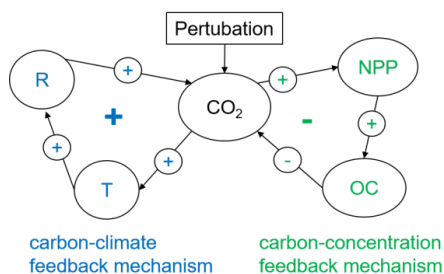
7 **Abstract.**

8 Earth system models simplify complex terrestrial respiration processes assuming a first-order chemical reaction or
9 assuming a Michaelis-Menten kinetics. The epistemic uncertainty related to the respective mathematical
10 representations is unclear. Using a simplified model of biogeochemical feedbacks to climate, we show that the
11 terrestrial carbon-climate feedback is more than 35% higher, and hence the remaining carbon budget to keep global
12 warming below 2 °C is 89-158 Pg C higher, when assuming Michaelis-Menten kinetics instead of first-order
13 kinetics, but these differences depend on the underlying emission scenario. These results show the importance of
14 an increased understanding of the mathematical model structure of respiration processes in Earth System Models
15 for more reliably projecting future carbon dynamics and climate, related feedback mechanisms, and hence to
16 estimate a valid remaining anthropogenic carbon budget.

17 **1 Introduction**

18 The anthropogenic emission of carbon dioxide into the atmosphere since the industrialization period led to a global
19 warming of about 1 K due to the greenhouse effect (Canadell et al., 2023). However, less than half of the
20 anthropogenically emitted carbon remains in the atmosphere because terrestrial ecosystems and the ocean take up
21 34% and 25%, respectively (Friedlingstein et al., 2023). The main reasons for this strong carbon dioxide uptake in
22 terrestrial ecosystems are biogeochemical feedbacks (Cox et al., 2000). Increasing atmospheric carbon dioxide
23 (CO₂) concentration leads to an enhanced photosynthesis rate, and hence to a CO₂ uptake by vegetation on land
24 (Cramer et al., 2001; O'sullivan et al., 2022) This carbon is stored in vegetation pools and ultimately transferred
25 to soils by exudation, litterfall, and mortality processes, thereby increasing the soil carbon content. This is the
26 important carbon-concentration feedback mechanism (Arneth et al., 2010) (Fig. 1) which is a negative feedback,
27 hence responsible for the current net CO₂ sink on land that has been preventing us from an even stronger climate
28 change. In contrast, autotrophic and heterotrophic respiration are also higher than under pre-industrial conditions
29 (Canadell et al., 2023) due to i) higher substrate availability and ii) the positive temperature sensitivity of
30 respiration (Lloyd and Taylor, 1994). This temperature sensitivity of respiration forms a positive carbon-climate
31 feedback mechanism (Fig. 1): Higher CO₂ concentration leads to higher temperature, which increases respiration
32 and hence leads to an even higher atmospheric CO₂ concentration (Arneth et al., 2010).

33



34

35 **Figure 1: Feedback diagram for two main terrestrial biogeochemical feedback mechanisms.** NPP: Net primary
 36 production, R: respiration, OC: land organic carbon stocks, T: global surface air temperature, CO₂: atmospheric
 37 carbon dioxide content.

38

39 These two biogeochemical feedback mechanisms have been identified as two major feedback mechanisms in the
 40 Earth system with great impact on climate (Friedlingstein et al., 2006; Arora et al., 2020). Currently, the positive
 41 carbon-climate feedback is lower than the negative carbon-concentration feedback and therefore land ecosystems
 42 act as a natural sink of CO₂ of about 3 Pg C per year (Friedlingstein et al., 2023). However, due to internal dynamics
 43 of the system, climate change, and changes in anthropogenic CO₂ emissions, the future strength of the feedback
 44 mechanisms and hence the net CO₂ exchange between land and atmosphere remains unclear. Recent accumulation
 45 of soil carbon in concert with higher future temperature and a declining increase in productivity can lead to a
 46 decreasing land sink under increasing CO₂ emissions in future (Cramer et al., 2001; Jones et al., 2023). To estimate
 47 such feedbacks, we need to run a modified version of an Earth System Model in which the direct effect of one
 48 system quantity on another is removed in a way that the feedback mechanism of question is not represented
 49 anymore. The temporal difference in atmospheric CO₂ concentration from such experiments to results of a control
 50 model run that incorporates all feedbacks is used to quantify these feedbacks (Zickfeld et al., 2011).

51 For the carbon-climate feedback mechanism (Fig. 1), the representation of respiration processes in Earth System
 52 Models is crucial. Several assumptions about the underlying processes and respective mathematical
 53 representations have been proposed. Land surface models usually represent respiration as a linear function (first-
 54 order kinetics) to the amount of available substrate (organic carbon, C),

$$55 \frac{dC}{dt} = -k \cdot C \quad (1)$$

56 using a different amount of carbon pools (Sitch et al., 2003; Brovkin et al., 2013; Tang et al., 2022), with
 57 decomposition rate constants k. However, the underlying biochemical reactions are mostly enzymatic, hence a
 58 Michaelis-Menten kinetics model should be more valid to represent the dynamics of respiration (Wieder et al.,
 59 2013; Yu et al., 2020)

$$60 \frac{dC}{dt} = v_{max} \frac{C}{K_M + C} \quad (2)$$

61 where v_{max} is the maximum reaction rate under infinite carbon substrate C , and K_M represents the amount of
 62 carbon at which the reaction rate is half of the maximum. The nonlinear shape of this relationship between reaction
 63 rate and substrate availability (in contrast to the linear dependency of first-order kinetics models) leads to a steep
 64 increase of the reaction rate under low substrate availability while only a moderate to negligible increase under
 65 high substrate availability. In doing so, this model implicitly represents the function of enzymes in the underlying
 66 biochemical reactions. Such model enables a more valid aggregation from the process level (e.g. rhizosphere,
 67 aggregatusphere) to the landscape scale (Reichstein and Beer, 2008).



68 The two approaches represented by equations 1 and 2 imply different responses of respiration to changing substrate
69 availability. Therefore, future dynamics of respiration should differ depending on the mathematical formulation.
70 Such structural model uncertainty is in particular of interest because there might be a point when the land sink
71 starts to decrease even under continuing high anthropogenic emissions (Cramer et al., 2001), or for the question
72 on how land sinks will react to decreasing or even negative anthropogenic carbon emissions.

73 Therefore, we ask three main questions in this paper: What is the effect of the respiration model structure on

- 74 • projections of the land carbon sink
- 75 • the strength of the carbon-climate feedback
- 76 • the remaining anthropogenic carbon budget

77 under different carbon emission scenarios? To address these questions we perform a full feedback analysis using
78 a simplified but process-based model of global biogeochemical feedback mechanisms twice, using a first-order
79 and a Michaelis-Menten kinetics model of respiration.

80 2 Methods

81 2.1 Simplified Carbon-Climate Feedback Model

82 The model has been designed to study the two major biogeochemical feedbacks to climate displayed in Fig. 1.
83 Exchanges of carbon among atmosphere, ocean and land are represented using a reduced number of carbon pools
84 without spatial details but still in a process-based way, i.e. based on a set of differential equations. For example,
85 the amount of carbon taken up by vegetation depends on the atmospheric carbon content while the amount of CO₂
86 released to the atmosphere due to respiration depends on the carbon content of the ecosystem. The model assumes
87 a global surface air temperature change due to changing atmospheric carbon dioxide content using a transient
88 climate response parameter, which is lagged due to the ocean heat capacity. The model has been driven by
89 anthropogenic carbon dioxide emissions to the atmosphere following several scenarios developed for the IPCC
90 6th assessment report.

91 A detailed description of the model can be found in (Lade et al., 2018). This model version has been revised in
92 terms of the land carbon pool dynamics. Here, we apply two alternative model versions, one assuming a first-order
93 kinetics of respiration (FOK), and one assuming a Michaelis-Menten kinetics of respiration (MMK). The
94 representation of terrestrial carbon uptake by gross primary productivity is identical in both model versions. It is
95 assumed to increase logarithmic with atmospheric carbon dioxide C_a (Equations 3 and 4, first term right-hand
96 side). In addition, emissions due to land use change E_L are subtracted the same way in both versions, and the
97 increase in respiration with temperature is represented by a typical Q_{10} model (Equations 3 and 4, second term
98 right-hand side). Only the dependence of respiration to land carbon stocks differs. The FOK model assumes a first-
99 order kinetics with a respiration rate constant estimated by pre-industrial GPP and carbon stocks, $k = \frac{GPP_0}{C_{L,0}}$
100 following the same principle as in (Lade et al., 2018).

$$101 \frac{dC_L}{dt} = GPP_0 \left(1 + \alpha \log \frac{C_a}{C_{a,0}} \right) - Q_{10}^{\frac{\Delta T}{10}} \cdot k \cdot C_L - E_L \quad (3)$$

102 In contrast, the MMK model represents respiration as a classical Michaelis-Menten equation with parameters v_{max}
103 and K_M :

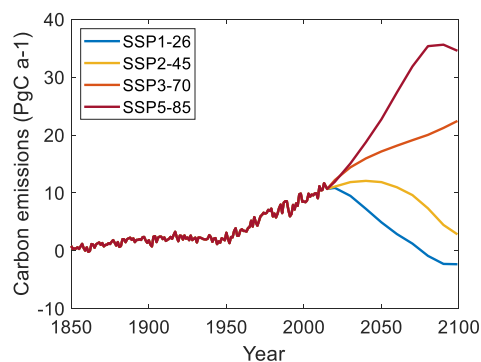


$$104 \quad \frac{dC_L}{dt} = GPP_0 \left(1 + \alpha \log \frac{C_a}{C_{a,0}} \right) - Q^{\frac{\Delta T}{10}} \cdot v_{max} \frac{C_L}{K_M + C_L} - E_L \quad (4)$$

105 2.2 Carbon emission scenarios

106 The models have been run from 1750 until 2100 forced by anthropogenic carbon dioxide emissions from fossil
 107 fuel burning and from land-use change. For this, we combined reported historical emissions from the Global
 108 Carbon Project (Friedlingstein et al., 2023) with Shared Socioeconomic Pathways (SSP) emission scenarios from
 109 the public database of the Institute for Applied Systems Analysis (Riahi et al., 2017). We selected four widely
 110 used scenarios produced for the CMIP6 protocol (Gidden et al., 2019): SSP1-26 (optimistic scenario, reaching
 111 economic growth while retaining sustainability and reducing inequalities), SSP2-45 (including mitigation
 112 strategies), SSP3-70 (represents a future of inequality and fossil fuel dependency), and SSP5-85 (representing
 113 economic growth through strong reliance on fossil fuels). These scenarios reach a forcing of 2.6, 4.5, 7.0, and 8.5
 114 W/m² at the end of the century and represent a huge spread of carbon emissions into the atmosphere (Fig. 2). We
 115 interpolated linearly the reported emissions at decadal scale to an annual resolution. In the combined time series
 116 (Fig. 2), historical emissions span the period 1850-2014 and scenarios continue from 2015 until 2100.

117



118

119 **Figure 2: Total CO₂ emissions from burning fossil fuels and land-use change from combining a historical dataset with**
 120 **results from Integrated Assessment Models for different scenarios.**

121

122 2.3 Feedback analysis and modelling protocol

123 We define the biogeochemical feedback following (Zickfeld et al., 2011) as the difference between two different
 124 temporal changes in atmospheric carbon dioxide content, one derived using a model including the feedback
 125 mechanism and using one neglecting such mechanism. For this, we averaged atmospheric CO₂ content during a
 126 reference period in the past (1850-1900), and one in the future (2080-2100). The difference between both periods
 127 is the carbon dioxide change. Then, we express the feedback in units of Pg C as the difference in carbon dioxide
 128 change between two distinct model runs: (i) the control model run which represents the feedback (“on”) and (ii) a
 129 model run which avoids the feedback mechanism (“off”). To disable the terrestrial carbon-climate feedback
 130 mechanism we set the parameter Q (Equations 3 and 4) to 1, i.e. any change in atmospheric temperature does not
 131 affect terrestrial ecosystem respiration in this model experiment. We performed these two model runs for both



132 model versions, FOK and MMK so that we can analyse the feedback separately, and then repeat all the procedure
 133 for all of the applied emission scenarios.

134 In addition, we calculate the feedback factor as the ratio of these temporal changes instead of the difference
 135 (Zickfeld et al., 2011; Lade et al., 2018). This measure is commonly used to compare the relative strength among
 136 various biogeochemical feedback mechanisms. It also shows if a positive or negative feedback is present.

137 The models run from 1850 until 2100 in a daily time step with CO₂ emission input interpolated from annual data.
 138 Parameters and pre-industrial pools and fluxes for model initialization were taken from (Lade et al., 2018) and
 139 partly adjusted (Table 1). The transient climate response to CO₂ doubling λ is set at the higher end of the range
 140 reported for CMIP6 model results (Nijssse et al., 2020; Arora et al., 2020) in order to match the observed historical
 141 temperature change. Parameters v_{max} and K_M of Equation 4 are set such that MMK model results match FOK
 142 model results for the pre-industrial period (cf. Fig. 3).

143

144 **Table 1. Value and description of parameters different from (Lade et al., 2018).**

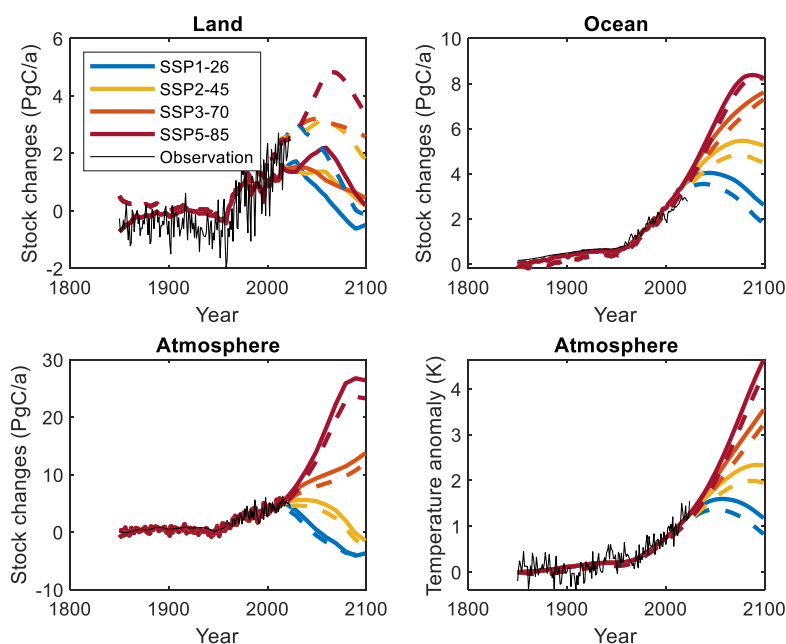
Name	Symbol	Value	Reference/comment
Pre-industrial soil and vegetation Carbon	$C_{L,0}$	2287 Pg C	Sum of vegetation and soils carbon stocks following (Canadell et al., 2023), and C stocks of the active layer of gelisols following (Hugelius et al., 2014)
Transient climate response to CO ₂ doubling (TCR)	λ (Equation 10 of (Lade et al., 2018))	2.5 K	Tuning parameter, higher end of range of CMIP6 models (Nijssse et al., 2020; Arora et al., 2020)
Respiration sensitivity parameter	Q	2	(Vaughn and Torn, 2019)
Pre-industrial GPP	GPP_0	113 Pg C / a	(Friedlingstein et al., 2023)
CO ₂ sensitivity of GPP	α	0.35	Tuning parameter, (Alexandrov et al., 2003)
Max respiration rate in MMK model	v_{max}	176 Pg C / a	Tuning parameter
Substrate concentration at half of max respiration rate in MMK model	K_M	1300 Pg C	Tuning parameter

145



146 **3 Results**

147 Model results of carbon stock changes and the surface temperature change for the historical time period are in
 148 general agreement with observations (Fig. 3), i.e. the overall historical trends are captured. The model does not
 149 represent spatial details, oversimplifies functional diversity and does not represent certain processes, such as
 150 disturbances. Therefore, the model is not able to capture the inter-annual variability of land carbon fluxes (Fig. 3).
 151 This general agreement shows that major biogeochemical feedback mechanisms are correctly represented, and that
 152 initial conditions (Table 1) and model parameters (Table 1) are reasonable. Therefore, we assume that we can
 153 apply this model to study the effects of structural respiration model uncertainty on the carbon-climate feedback
 154 strength.
 155

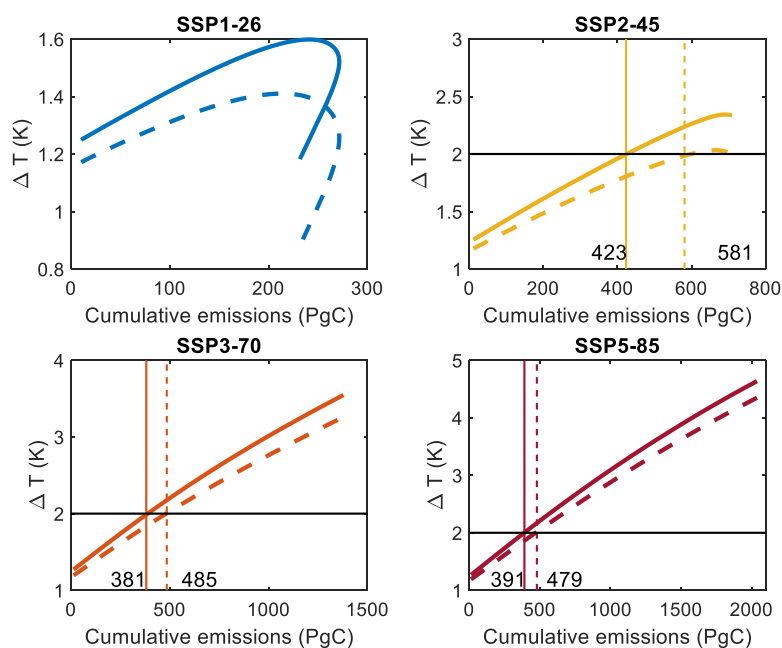


156
 157 **Figure 3: Simulated carbon stock changes and temperature anomaly for the different scenarios. MMK model results**
 158 **are displayed by dashed lines. Simulation results are compared to estimates by the Global Carbon Project or to the**
 159 **NOAA Global Surface Temperature record, which has been bias corrected to the model results to match reference**
 160 **periods.**

161
 162 Figure 3 also shows the projections of carbon fluxes to land, ocean and atmosphere, as well as the temperature
 163 change for the two different model structures until 2100 following the different emission scenarios. Overall, these
 164 projections of the main carbon cycle fluxes and temperature change are similar to concentration-driven CMIP6
 165 results (Canadell et al., 2023). Our projected ocean carbon sink is substantially higher for most of the scenarios,
 166 and the land carbon sink of the model using a first-order kinetics respiration approach (FOK) is lower, but
 167 comparable with (Lade et al., 2018). Otherwise, the projections of the change in atmospheric carbon stocks and
 168 the global surface temperature change are similar to studies using Earth System Models (Canadell et al., 2023).



169 However, spread of carbon cycle projections using other models is usually also very high (Canadell et al., 2023),
 170 and the uncertainty due to parameter values or initial conditions hardly quantified in these studies.
 171 The projected land sink evolution differs depending on both, the emission scenario and the model structure applied.
 172 Under high emission scenarios, the land sink continues to rise and peaks in the middle of the century followed by
 173 a decreasing sink until 2100. This peak has been reported by DGVMs and ESMs before (Cramer et al., 2001; Jones
 174 et al., 2023) and is due to the reverse shape of the two main response functions, logarithmic productivity response
 175 to elevated CO₂ and quasi-exponential respiration response to temperature. A second reason is internal carbon
 176 dynamics: Respiration depends on the amount of land carbon stocks, which continued to increase until some
 177 maximum and therefore is the basis for a high respiration flux during the following time. For the scenario SSP1-
 178 26, the land sink starts to decrease immediately after the historical period, i.e. when emissions are reduced, and
 179 depending on the model structure is getting even negative at the second half of the century.
 180 The projected land carbon sink in 2100 is much higher when assuming a Michaelis-Menten kinetics model for
 181 respiration (MMK) even under an equal temperature sensitivity of respiration as by the first-order kinetics model
 182 (FOK), and even when parameters are chosen to fit both model results during the historical period. In addition, the
 183 peak in the middle of the century is more pronounced when using the MMK model (Fig. 3). Hence, this difference
 184 is only due to internal carbon dynamics differences, in particular a non-linear (decreasing) change of the respiration
 185 rate with increasing substrate availability under when assuming Michaelis-Menten kinetics. This clearly
 186 demonstrates the uncertainty of land carbon sink dynamics just due to alternative assumptions and mathematical
 187 formulations of respiration processes. As a result of higher land sinks using the MMK model, ocean and
 188 atmosphere sinks are smaller and the temperature change is lower (Fig. 3). Due to the higher land C sink assuming
 189 Michaelis-Menten kinetics, also total changes in land carbon stocks are much higher, i.e. land takes up several
 190 hundred of Pg C more depending on the emission scenario.



191



192 **Figure 4.** Relationship between global air surface temperature difference to pre-industrial temperature and the cumulative
 193 emission of CO₂ from 2024 until 2099 for different emission scenarios and the two model simulations FOK (solid lines) and
 194 MMK (dashed lines). Horizontal lines indicate a temperature change threshold of 2K, and vertical lines and numbers indicate
 195 the respective cumulative emissions since 2024 to reach that temperature change target.

196

197 These differences in the projected land sinks do have clear consequences for the Transient Climate Response to
 198 Cumulative Emissions of Carbon Dioxide (TCRE) and hence the remaining anthropogenic carbon budgets under
 199 different emission scenarios. Usually, there is a quasi-linear relationship between the cumulative emission and the
 200 temperature change (Fig. 4). Under reduced emissions of SSP1-26 scenario, ocean and land C uptake may remain
 201 high (blue curves in Fig. 3), leading to a hysteresis in the TCRE (Koven et al., 2023). Such hysteresis is not visible
 202 in the other scenarios (Fig. 4) because emission reductions are not strong enough (Fig. 2). Interestingly, the
 203 relationship is less steep and more non-linear for the MMK model for all scenarios. From the TCRE the remaining
 204 carbon budget for a certain temperature threshold can be estimated (Canadell et al., 2023). In Fig. 4, the vertical
 205 lines indicate the amount of emissions since 2024 that - according to this model - can be still emitted in order to
 206 keep warming below the threshold of 2 °C warming compared to the pre-industrial situation, which is indicated
 207 by the horizontal line. We skip this analysis for scenario SSP1-26 results because the MMK model fails to reach
 208 a 2 °C increase at all (Fig. 4). For the other emission scenarios, the FOK model suggests 381 to 423 Pg C that can
 209 be emitted to the atmosphere in order to keep warming below 2 °C compared to pre-industrial temperature (Fig.
 210 4). These estimates are slightly higher than the median remaining C budget estimated by CMIP6 experiments using
 211 ESMs of 370 Pg C (table 5.8, (Canadell et al., 2023)). Importantly, when assuming a Michaelis-Menten kinetics
 212 of respiration (MMK), the remaining C budget is higher and range between 479-581 Pg C. This is due to flatter
 213 slopes of these model results (Fig. 4).

214

215 **Table 2.** Terrestrial carbon-climate feedback (Pg C) for different representations of respiration in the model.
 216 Shown is the difference of model results accounting for the feedback and excluding it based on the temporal change
 217 in atmospheric carbon content between 2080-2100 and 1850-1900.

	First-order kinetics (FOK)	Michaelis-Menten kinetics (MMK)	relative difference (%)
SSP1-26	74	101	37
SSP2-45	163	221	36
SSP3-70	262	365	39
SSP5-85	380	534	40

218

219 Using the first-order kinetics approach of respiration (FOK), we estimate a carbon-climate feedback of 74 to 380
 220 Pg C when comparing the average CO₂ concentration of the period 2080-2100 with pre-industrial conditions,
 221 depending on the emission scenario (Table 2). This translates into a mean feedback factor of 1.42 with a small
 222 range (Fig. 5) (Table 3), which are similar to previous estimates (Lade et al., 2018). Interestingly, the strength of
 223 the feedback mechanism as expressed by the feedback factor decreases with increasing carbon emissions (Table
 224 3), i.e. the internal Earth system interactions are more important under reduced anthropogenic emissions. However,
 225 when assuming Michaelis-Menten kinetics of respiration, this carbon-climate feedback is even 36-40% higher
 226 (Table 2, Fig. 5) depending on the underlying scenario. While the absolute feedback difference increases with the



227 amount of anthropogenic carbon emissions (Table 2), the relative difference of the feedback factor decreases from
 228 63% (SSP1-26) to 26% (SSP5-85) (Table 3).

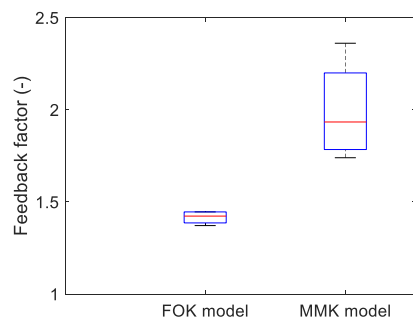
229

230 **Table 3.** Feedback factor of the terrestrial carbon-climate feedback for different representations of respiration in
 231 the model. Shown is the difference of model results accounting for the feedback and excluding it based on the
 232 temporal change in atmospheric carbon content between 2080-2100 and 1850-1900.

	First-order kinetics (FOK)	Michaelis-Menten kinetics (MMK)	relative difference (%)
SSP1-26	1.45	2.36	63
SSP2-45	1.45	2.03	41
SSP3-70	1.4	1.82	30
SSP5-85	1.37	1.73	26

233

234



235

236 **Figure 5** Distribution of the feedback factor for the two model versions FOK and MMK across emission scenarios based on
 237 the temporal change in atmospheric carbon content between 2080-2100 and 1850-1900.

238 4 Discussion

239 Besides gross primary productivity, ecosystem respiration is one of the main land-atmosphere carbon exchange
 240 processes (Friedlingstein et al., 2023). The underlying biochemical processes are complex and mathematical
 241 models of simplified net reactions are usually applied in Earth System Models: Either assuming a first-order
 242 chemical reaction of carbon and oxygen to carbon dioxide and applying Equation 1, or considering the underlying
 243 enzymatic reactions and hence applying Equation 2. The epistemic uncertainty in projecting future land-
 244 atmosphere exchange of CO₂, climate and the related biogeochemical feedbacks underlying these assumptions
 245 have been addressed in this paper. Model parameters have been chosen based on literature values, and to fit
 246 historical carbon and temperature changes (section 2.3) for the first-order kinetics approach (FOK).

247 For the Michaelis-Menten kinetics model (MMK), we selected parameter values such that results are similar to the
 248 FOK model during the pre-industrial period. Interestingly, effects of anthropogenic carbon emissions on future
 249 land sink dynamics differ between both model versions, with several Pg C per year higher uptake by land when
 250 assuming Michaelis-Menten kinetics for respiration (Fig. 3). Such higher land carbon uptake leads to a lower ocean
 251 carbon sink hence increasing differences between land and ocean sinks. In addition, the projected global surface
 252 temperature change until 2100 is lower in the MMK model (Fig. 3), i.e. a lower temperature change response to



253 cumulative carbon emissions (Fig. 4). Since increasing surface temperature will lead to an additional CO₂ release
254 from land to the atmosphere, there is the positive carbon-climate feedback mechanism (Arneth et al., 2010) and we
255 asked the question, is there also an effect of the respiration model structure on this feedback strength?
256 Indeed, this feedback is more than 35 % higher when assuming Michaelis-Menten kinetics, and it is higher for
257 strong carbon emission scenarios (Table 2). As a consequence, our results imply a 88 Pg C (SSP5-85) to 158 Pg
258 C (SSP2-45) higher remaining anthropogenic carbon budget to keep warming below 2 °C above pre-industrial
259 levels only because we assume an alternative model structure for respiration. These estimates are of the same order
260 of magnitude but substantially higher than estimates of additional warming-induced C loss from permafrost-
261 affected soils until 2100 of 10-100 Pg C (Koven et al., 2015). Other additional Earth system feedbacks currently
262 not represented in Earth system models (section 5.5.2.2.5 in (Canadell et al., 2023)), and additional Geophysical
263 Uncertainties like non- CO₂ forcing or emission uncertainty (Table 5.8 in (Canadell et al., 2023)) are also of the
264 same order of magnitude .
265 We applied a simplified model of global biogeochemical feedback mechanisms, considering only one terrestrial
266 carbon pool and no explicit pool of microbial biomass and microbial functions. Therefore, many specific
267 underlying processes and interactions of ecosystem components are neglected. For example, an increase in
268 respiration due to increasing plant productivity and carbon input to soils (priming effect, (Fontaine et al., 2007;
269 Keuper et al., 2020)), or changing microbial community structure as a response to climate change (Glassman et
270 al., 2018) is not considered. Nutrient limitations of vegetation productivity (Hungate et al., 2003) is only implicitly
271 parametrized in Equations 3 and 4. In addition, climate change is expressed as a temperature change in this model
272 and precipitation effects on carbon cycle functions (Jung et al., 2017) are not taken into account. We therefore see
273 our results as first conservative estimates that point to the importance to communicate and address existing
274 structural uncertainties in Earth System Models. Just by assuming an underlying Michaelis-Menten kinetics of
275 respiration processes leads to distinct projections of future respiration and the carbon-climate feedback mechanism.
276 These results also demonstrate the need for novel research clarifying a valid process-based model structure of
277 ecosystem respiration.

278 **5 Conclusions**

279 Two major gross carbon fluxes govern the recent land carbon sink, photosynthesis and respiration. While detailed
280 process-based photosynthesis models have been developed and applied in Earth System Models, how to model
281 respiration processes remains unclear. The model structure of respiration alone leads to a relative difference in the
282 carbon-climate feedback over the 21st century of more than 35%. Depending on the underlying emission scenario,
283 that translates into a difference of the remaining carbon budget to keep global warming below 2 °C of 89 Pg C
284 (SSP5-85) to 158 Pg C (SSP2-45). These results show the importance of an increased understanding of the
285 mathematical model structure of respiration processes in Earth System Models for more reliably projecting future
286 carbon dynamics and climate, related feedback mechanisms, and hence to estimate a valid remaining
287 anthropogenic carbon budget.

288

289

290 **Code availability**

291 MATLAB code of the model versions applied will be made available via github after publication.



292

293 **Data availability**

294 All required data to run the model and reproduce the results is available online and open access.

295

296 **Author contribution** CB designed the study, wrote the computer code, downloaded and interpolated the emission
297 data, run the models, analysed the results and wrote the manuscript.

298

299 **Competing interests** CB declares that he has no conflict of interest.

300 **Acknowledgements** CB acknowledges financial support by Deutsche Forschungsgemeinschaft through the
301 Heisenberg program (508047523).

302 **References**

303 Alexandrov, G. A., Oikawa, T., and Yamagata, Y.: Climate dependence of the CO₂ fertilization effect on terrestrial
304 net primary production, *Tellus Series B-Chemical and Physical Meteorology*, 55, 669-675, DOI 10.1034/j.1600-
305 0889.2003.00021.x, 2003.

306 Arneeth, A., Harrison, S. P., Zaehle, S., Tsigaridis, K., Menon, S., Bartlein, P. J., Feichter, J., Korhola, A., Kulmala,
307 M., O'Donnell, D., Schurgers, G., Sorvari, S., and Vesala, T.: Terrestrial biogeochemical feedbacks in the climate
308 system, *Nature Geoscience*, 3, 525-532, 10.1038/ngeo905, 2010.

309 Arora, V. K., Katavouta, A., Williams, R. G., Jones, C. D., Brovkin, V., Friedlingstein, P., Schwinger, J., Bopp, L.,
310 Boucher, O., Cadule, P., Chamberlain, M. A., Christian, J. R., Delire, C., Fisher, R. A., Hajima, T., Ilyina, T.,
311 Joetjzer, E., Kawamiya, M., Koven, C. D., Krasting, J. P., Law, R. M., Lawrence, D. M., Lenton, A., Lindsay, K.,
312 Pongratz, J., Raddatz, T., Séférian, R., Tachiiri, K., Tjiputra, J. F., Wiltshire, A., Wu, T., and Ziehn, T.: Carbon-
313 concentration and carbon-climate feedbacks in CMIP6 models and their comparison to CMIP5 models,
314 *Biogeosciences*, 17, 4173-4222, 10.5194/bg-17-4173-2020, 2020.

315 Brovkin, V., Boysen, L., Raddatz, T., Gayler, V., Loew, A., and Claussen, M.: Evaluation of vegetation cover and
316 land-surface albedo in MPI-ESM CMIP5 simulations, *Journal of Advances in Modeling Earth Systems*, 5, 48-57,
317 <https://doi.org/10.1029/2012MS000169>, 2013.

318 Canadell, J. G., Monteiro, P. M. S., Costa, M. H., Cotrim da Cunha, L., Cox, P. M., Eliseev, A. V., Henson, S., Ishii,
319 M., Jaccard, S., Koven, C., Lohila, A., Patra, P. K., Piao, S., Rogelj, J., Syampungani, S., Zaehle, S., and Zickfeld,
320 K.: Global Carbon and Other Biogeochemical Cycles and Feedbacks, in: *Climate Change 2021 – The Physical
321 Science Basis: Working Group I Contribution to the Sixth Assessment Report of the Intergovernmental Panel on
322 Climate Change*, edited by: Intergovernmental Panel on Climate, C., Cambridge University Press, Cambridge,
323 673-816, DOI: 10.1017/9781009157896.007, 2023.

324 Cox, P. M., Betts, R. A., Jones, C. D., Spall, S. A., and Totterdell, I. J.: Acceleration of global warming due to carbon-
325 cycle feedbacks in a coupled climate model, *Nature*, 408, 184-187, 2000.

326 Cramer, W., Bondeau, A., Woodward, F. I., Prentice, I. C., Betts, R. A., Brovkin, V., Cox, P. M., Fisher, V., Foley,
327 J. A., Friend, A. D., Kucharik, C., Lomas, M. R., Ramankutty, N., Sitch, S., Smith, B., White, A., and Young-
328 Molling, C.: Global response of terrestrial ecosystem structure and function to CO₂ and climate change: results
329 from six dynamic global vegetation models, *Global change biology*, 7, 357-373, 2001.



- 330 Fontaine, S., Barot, S., Barré, P., Bdioui, N., Mary, B., and Rumpel, C.: Stability of organic carbon in deep soil layers
331 controlled by fresh carbon supply, *Nature*, 450, 277-U210, 10.1038/nature06275, 2007.
- 332 Friedlingstein, P., Cox, P., Betts, R., Bopp, L., Von Bloh, W., Brovkin, V., Cadule, P., Doney, S., Eby, M., Fung, I.,
333 Bala, G., John, J., Jones, C., Joos, F., Kato, T., Kawamiya, M., Knorr, W., Lindsay, K., Matthews, H. D., Raddatz,
334 T., Rayner, P., Reick, C., Roeckner, E., Schnitzler, K. G., Schnur, R., Strassmann, K., Weaver, A. J., Yoshikawa,
335 C., and Zeng, N.: Climate-carbon cycle feedback analysis: Results from the C⁴MIP model intercomparison, *Journal*
336 *of Climate*, 19, 3337-3353, 2006.
- 337 Friedlingstein, P., O'Sullivan, M., Jones, M. W., Andrew, R. M., Bakker, D. C. E., Hauck, J., Landschützer, P., Le
338 Quéré, C., Luijkx, I. T., Peters, G. P., Peters, W., Pongratz, J., Schwingshackl, C., Sitch, S., Canadell, J. G., Ciais,
339 P., Jackson, R. B., Alin, S. R., Anthoni, P., Barbero, L., Bates, N. R., Becker, M., Bellouin, N., Decharme, B.,
340 Bopp, L., Brasika, I. B. M., Cadule, P., Chamberlain, M. A., Chandra, N., Chau, T. T. T., Chevallier, F., Chini, L.
341 P., Cronin, M., Dou, X., Enyo, K., Evans, W., Falk, S., Feely, R. A., Feng, L., Ford, D. J., Gasser, T., Ghattas, J.,
342 Gkritzalis, T., Grassi, G., Gregor, L., Gruber, N., Gürses, Ö., Harris, I., Hefner, M., Heinke, J., Houghton, R. A.,
343 Hurtt, G. C., Iida, Y., Ilyina, T., Jacobson, A. R., Jain, A., Jarníková, T., Jersild, A., Jiang, F., Jin, Z., Joos, F.,
344 Kato, E., Keeling, R. F., Kennedy, D., Klein Goldewijk, K., Knauer, J., Korsbakken, J. I., Körtzinger, A., Lan, X.,
345 Lefèvre, N., Li, H., Liu, J., Liu, Z., Ma, L., Marland, G., Mayot, N., McGuire, P. C., McKinley, G. A., Meyer, G.,
346 Morgan, E. J., Munro, D. R., Nakaoka, S. I., Niwa, Y., O'Brien, K. M., Olsen, A., Omar, A. M., Ono, T., Paulsen,
347 M., Pierrot, D., Pockock, K., Poulter, B., Powis, C. M., Rehder, G., Resplandy, L., Robertson, E., Rödenbeck, C.,
348 Rosan, T. M., Schwinger, J., Séférian, R., Smallman, T. L., Smith, S. M., Sospedra-Alfonso, R., Sun, Q., Sutton,
349 A. J., Sweeney, C., Takao, S., Tans, P. P., Tian, H., Tilbrook, B., Tsujino, H., Tubiello, F., van der Werf, G. R.,
350 van Ooijen, E., Wanninkhof, R., Watanabe, M., Wimart-Rousseau, C., Yang, D., Yang, X., Yuan, W., Yue, X.,
351 Zaehle, S., Zeng, J., and Zheng, B.: Global Carbon Budget 2023, *Earth Syst. Sci. Data*, 15, 5301-5369,
352 10.5194/essd-15-5301-2023, 2023.
- 353 Gidden, M. J., Riahi, K., Smith, S. J., Fujimori, S., Luderer, G., Kriegler, E., van Vuuren, D. P., van den Berg, M.,
354 Feng, L., Klein, D., Calvin, K., Doelman, J. C., Frank, S., Fricko, O., Harmsen, M., Hasegawa, T., Havlik, P.,
355 Hilaire, J., Hoesly, R., Horing, J., Popp, A., Stehfest, E., and Takahashi, K.: Global emissions pathways under
356 different socioeconomic scenarios for use in CMIP6: a dataset of harmonized emissions trajectories through the
357 end of the century, *Geosci. Model Dev.*, 12, 1443-1475, 10.5194/gmd-12-1443-2019, 2019.
- 358 Glassman, S. I., Weihe, C., Li, J. H., Albright, M. B. N., Looby, C. I., Martiny, A. C., Treseder, K. K., Allison, S.
359 D., and Martiny, J. B. H.: Decomposition responses to climate depend on microbial community composition, *P*
360 *Natl Acad Sci USA*, 115, 11994-11999, 10.1073/pnas.1811269115, 2018.
- 361 Hugelius, G., Strauss, J., Zubrzycki, S., Harden, J. W., Schuur, E. A. G., Ping, C.-L., Schirrmeister, L., Grosse, G.,
362 Michaelson, G. J., Koven, C. D., O'Donnell, J. A., Elberling, B., Mishra, U., Camill, P., Yu, Z., Palmtag, J., and
363 Kuhry, P.: Estimated stocks of circumpolar permafrost carbon with quantified uncertainty ranges and identified
364 data gaps, *Biogeosciences*, 11, 6573-6593, 10.5194/bg-11-6573-2014, 2014.
- 365 Hungate, B. A., Dukes, J. S., Shaw, M. R., Luo, Y. Q., and Field, C. B.: Nitrogen and climate change, *Science*, 302,
366 1512-1513, DOI 10.1126/science.1091390, 2003.
- 367 Jones, C. D., Ziehn, T., Anand, J., Bastos, A., Burke, E., Canadell, J. G., Cardoso, M., Ernst, Y., Jain, A. K., Jeong,
368 S., Keller, E. D., Kondo, M., Lauerwald, R., Lin, T. S., Murray-Tortarolo, G., Nabuurs, G. J., O'Sullivan, M.,
369 Poulter, B., Qin, X. Y., von Randow, C., Sanches, M., Schepaschenko, D., Shvidenko, A., Smallman, T. L., Tian,



- 370 H. Q., Villalobos, Y., Wang, X. H., and Yun, J. M.: RECCAP2 Future Component: Consistency and Potential for
371 Regional Assessment to Constrain Global Projections, *Agu Adv*, 4, ARTN e2023AV001024
372 10.1029/2023AV001024, 2023.
- 373 Jung, M., Reichstein, M., Schwalm, C. R., Huntingford, C., Sitch, S., Ahlström, A., Arneth, A., Camps-Valls, G.,
374 Ciais, P., Friedlingstein, P., Gans, F., Ichii, K., Ain, A. K. J., Kato, E., Papale, D., Poulter, B., Raduly, B.,
375 Rödenbeck, C., Tramontana, G., Viovy, N., Wang, Y. P., Weber, U., Zaehle, S., and Zeng, N.: Compensatory
376 water effects link yearly global land CO
377 sink changes to temperature, *Nature*, 541, 516-520, 10.1038/nature20780, 2017.
- 378 Keuper, F., Wild, B., Kummu, M., Beer, C., Blume-Werry, G., Fontaine, S., Gavazov, K., Gentsch, N.,
379 Guggenberger, G., Hugelius, G., Jalava, M., Koven, C., Krab, E. J., Kuhry, P., Monteux, S., Richter, A., Shahzad,
380 T., Weedon, J. T., and Dorrepaal, E.: Carbon loss from northern circumpolar permafrost soils amplified by
381 rhizosphere priming, *Nature Geoscience*, 13, 560-565, 10.1038/s41561-020-0607-0, 2020.
- 382 Koven, C. D., Sanderson, B. M., and Swann, A. L. S.: Much of zero emissions commitment occurs before reaching
383 net zero emissions, *Environmental Research Letters*, 18, 014017, 10.1088/1748-9326/acab1a, 2023.
- 384 Koven, C. D., Schuur, E. A. G., Schädel, C., Bohn, T. J., Burke, E. J., Chen, G., Chen, X., Ciais, P., Grosse, G.,
385 Harden, J. W., and et al.: A simplified, data-constrained approach to estimate the permafrost carbon-climate
386 feedback, *Philosophical Transactions of the Royal Society A: Mathematical, Physical and Engineering Sciences*,
387 373, 20140423-20140423, 2015.
- 388 Lade, S. J., Donges, J. F., Fetzer, I., Anderies, J. M., Beer, C., Cornell, S. E., Gasser, T., Norberg, J., Richardson, K.,
389 Rockström, J., and Steffen, W.: Analytically tractable climate--carbon cycle feedbacks under 21st century
390 anthropogenic forcing, *Earth System Dynamics*, 9, 507-523, 2018.
- 391 Lloyd, J. and Taylor, J. A.: On the temperature dependence of soil respiration, *Functional Ecology*, 8, 315-323, 1994.
- 392 Nijssse, F. J. M. M., Cox, P. M., and Williamson, M. S.: Emergent constraints on transient climate response (TCR)
393 and equilibrium climate sensitivity (ECS) from historical warming in CMIP5 and CMIP6 models, *Earth System
394 Dynamics*, 11, 737-750, 10.5194/esd-11-737-2020, 2020.
- 395 O'Sullivan, M., Friedlingstein, P., Sitch, S., Anthoni, P., Arneth, A., Arora, V. K., Bastrikov, V., Delire, C., Goll, D.
396 S., Jain, A., Kato, E., Kennedy, D., Knauer, J., Lienert, S., Lombardozzi, D., McGuire, P. C., Melton, J. R., Nabel,
397 J. E. M. S., Pongratz, J., Poulter, B., Séférian, R., Tian, H. Q., Vuichard, N., Walker, A. P., Yuan, W. P., Yue, X.,
398 and Zaehle, S.: Process-oriented analysis of dominant sources of uncertainty in the land carbon sink, *Nature
399 Communications*, 13, ARTN 4781
400 10.1038/s41467-022-32416-8, 2022.
- 401 Reichstein, M. and Beer, C.: Soil respiration across scales: the importance of a model--data integration framework
402 for data interpretation, *Journal of Plant Nutrition and Soil Science*, 171, 344-354, 2008.
- 403 Riahi, K., van Vuuren, D. P., Kriegler, E., Edmonds, J., O'Neill, B. C., Fujimori, S., Bauer, N., Calvin, K., Dellink,
404 R., Fricko, O., Lutz, W., Popp, A., Cuaresma, J. C., Samir, K. C., Leimbach, M., Jiang, L., Kram, T., Rao, S.,
405 Emmerling, J., Ebi, K., Hasegawa, T., Havlik, P., Humpenöder, F., Silva, L. A. D., Smith, S., Stehfest, E., Bosetti,
406 V., Eom, J., Gernaat, D., Masui, T., Rogelj, J., Strefler, J., Drouet, L., Krey, V., Luderer, G., Harmsen, M.,
407 Takahashi, K., Baumstark, L., Doelman, J. C., Kainuma, M., Klimont, Z., Marangoni, G., Lotze-Campen, H.,
408 Obersteiner, M., Tabeau, A., and Tavoni, M.: The Shared Socioeconomic Pathways and their energy, land use,
409 and greenhouse gas emissions implications: An overview, *Global Environmental Change*, 42, 153-168, 2017.



- 410 Sitch, S., Smith, B., Prentice, I. C., Arneth, A., Bondeau, A., Cramer, W., Kaplan, J. O., Levis, S., Lucht, W., Sykes,
411 M. T., and others: Evaluation of ecosystem dynamics, plant geography and terrestrial carbon cycling in the LPJ
412 dynamic global vegetation model, *Global Change Biology*, 9, 161-185, 2003.
- 413 Tang, J., Riley, W. J., and Zhu, Q.: Supporting hierarchical soil biogeochemical modeling: version 2 of the
414 Biogeochemical Transport and Reaction model (BeTR-v2), *Geosci. Model Dev.*, 15, 1619-1632, 10.5194/gmd-
415 15-1619-2022, 2022.
- 416 Vaughn, L. J. S. and Torn, M. S.: C evidence that millennial and fast-cycling soil carbon are equally sensitive to
417 warming, *Nature Climate Change*, 9, 467-+, 10.1038/s41558-019-0468-y, 2019.
- 418 Wieder, W. R., Bonan, G. B., and Allison, S. D.: Global soil carbon projections are improved by modelling microbial
419 processes, *Nature Climate Change*, 3, 909-912, 10.1038/nclimate1951, 2013.
- 420 Yu, L., Ahrens, B., Wutzler, T., Schrumpf, M., and Zaehle, S.: Jena Soil Model (JSM v1.0; revision 1934): a
421 microbial soil organic carbon model integrated with nitrogen and phosphorus processes, *Geoscientific Model
422 Development*, 13, 783-803, 10.5194/gmd-13-783-2020, 2020.
- 423 Zickfeld, K., Eby, M., Matthews, H. D., Schmittner, A., and Weaver, A. J.: Nonlinearity of Carbon Cycle Feedbacks,
424 *Journal of Climate*, 24, 4255-4275, <https://doi.org/10.1175/2011JCLI3898.1>, 2011.

425

426